The Annals of Applied Statistics
2016, Vol. 10, No. 4, 2182–2202
DOI: 10.1214/16-AOAS970

DYNAMIC SOCIAL NETWORKS BASED ON MOVEMENT[1]

BY HENRY R. SCHARF[*], MEVIN B. HOOTEN[†,*], BAILEY K. FOSDICK[*], DEVIN S. JOHNSON[‡], JOSH M. LONDON[‡] AND JOHN W. DURBAN[§]

Colorado State University[*], U.S. Geological Survey, Colorado Cooperative Fish and Wildlife Research Unit[†], NOAA Alaska Fisheries Science Center[‡] and NOAA Southwest Fisheries Science Center[§]

Network modeling techniques provide a means for quantifying social structure in populations of individuals. Data used to define social connectivity are often expensive to collect and based on case-specific, *ad hoc* criteria. Moreover, in applications involving animal social networks, collection of these data is often opportunistic and can be invasive. Frequently, the social network of interest for a given population is closely related to the way individuals move. Thus, telemetry data, which are minimally invasive and relatively inexpensive to collect, present an alternative source of information. We develop a framework for using telemetry data to infer social relationships among animals. To achieve this, we propose a Bayesian hierarchical model with an underlying dynamic social network controlling movement of individuals via two mechanisms: an attractive effect and an aligning effect. We demonstrate the model and its ability to accurately identify complex social behavior in simulation, and apply our model to telemetry data arising from killer whales. Using auxiliary information about the study population, we investigate model validity and find the inferred dynamic social network is consistent with killer whale ecology and expert knowledge.

1. Introduction. Dynamic social networks are an important topic of study among ecologists for a variety of species and ecological processes [Croft, James and Krause (2008), Krause, Croft and James (2007), Pinter-Wollman et al. (2013), Sih, Hanser and McHugh (2009), Wey et al. (2008)]. Social networks can help explain a myriad of behavioral activities in a population, including the characteristics of animal movement. Therefore, it is common to define social networks based on directly observable behavior such as the duration of time animals spend in close proximity to one another (e.g., African elephants, *Loxodonta africana* [Goldenberg et al. (2014)]), discrete counts of interactions (e.g., yellow (*Papio cynocephalus*) and anubis baboons (*Papio anubis*) [Franz et al. (2015)]), or discrete counts of close encounters (e.g., barn swallows (*Hirundo rustica erythrogaster*) [Levin et al. (2015)]). Challenges for researchers interested in studying animal social networks

Received January 2016; revised August 2016.
[1]Supported in part by NOAA ACK 188000 and NSF SES-1461495 and DMS-16-14392.
Key words and phrases. Dynamic social network, animal movement, *Orcinus orca*, hidden Markov model, Gaussian Markov random field.

include expensive data collection procedures and potential biases due to opportunistic observation.

Killer whales (*Orcinus orca*), like many marine mammals, are complex and highly social creatures [Baird and Whitehead (2000), Parsons et al. (2009), Pitman and Durban (2012), Williams and Lusseau (2006)]. To better understand the behavior of killer whales, we seek to characterize their social relationships. Unfortunately, direct observation of killer whale interactions is challenging; it is not uncommon for individuals to travel 50 km a day and to range over thousands of kilometers in a season [Andrews, Pitman and Ballance (2008), Durban and Pitman (2012)]. Furthermore, observation of killer whales at close proximity has been found to significantly influence their movement behavior [Williams, Trites and Bain (2002)], which could directly affect measurements of social connectivity. In contrast, satellite tracking tags have been used to gather movement data for killer whales over several months [Andrews, Pitman and Ballance (2008), Durban and Pitman (2012)], and there is little evidence to suggest that tags alter behavior. Thus, a potential alternative to costly personal observations are telemetry data, which contain rich movement information at the individual level and can be collected in remote areas at a much lower cost.

The suite of models for animal telemetry data is vast and rapidly changing, including both continuous- and discrete-time approaches [see McClintock et al. (2014) for a review]. Yet there are only a few models that explicitly account for interactions among individuals in the population [e.g., Codling and Bode (2014), Langrock et al. (2014), Morales et al. (2010), Russell, Hanks and Haran (2015)]. Moreover, methods are lacking that attempt to characterize pairwise connections between all members of the population. We propose a model for movement that incorporates plausible mechanistic effects on movement due to an underlying social network. Our model allows us to infer the specific characteristics of interaction in a given population and the underlying dynamic social network itself.

In our proposed discrete-time continuous-space model, we assume there exists an underlying (latent) dynamic social network among the individuals in the population. Conditional on the network characteristics and the positions of animals in the previous time step, the expected positions of individuals at the next time point are modeled jointly using a Gaussian Markov random field (GMRF) [Besag (1974), Besag and Kooperberg (1995), Rue and Held (2005)]. The model is temporally Markovian for both the animal positions and the social network. In our model, the underlying social structure influences movement through two channels: an attractive effect and an alignment effect. These channels of interaction allow us to model a wide variety of behaviors, and they have a precedent for use in the context of interaction behavior [Lemasson, Anderson and Goodwin (2013)]. The connection between the underlying social network and position is an example of a hidden Markov model (HMM). HMMs represent a flexible class of hierarchical models popular in analyses of wildlife data [see, e.g., Langrock et al. (2012)] in which an

observable process (in our case, position) is driven by an unobserved Markovian process (the underlying social network).

We introduce the details of our proposed method in Section 2. We demonstrate and assess inference from the model with simulated data in Section 3. In Section 4, we analyze data for seven killer whales tagged concurrently near the coast of the Antarctic Peninsula. Within the tagged sample, there are three genetically distinct types of killer whales [Morin et al. (2015), Pitman and Ensor (2003)] characterized by their size, coloration and diet. The spatial distributions for each type overlap, and while strong social interaction is typical within each type, there have been no observed social associations among animals of different types. We demonstrate that inferences from our method are consistent with this history of observation. Furthermore, we find strong evidence for dynamic social connections forming and dissolving within each type, but no indication of connections between types. Finally, in Section 5, we discuss potential extensions for the model, including the incorporation of environmental covariates and approaches for mediating the large computational demands for the model when the study sample is large.

2. Methods. We propose new methodology based on a general hierarchical modeling framework that accommodates measurement, process and parameter uncertainty [Berliner (1996)]. We introduce the GMRF that describes animal movement in Section 2.1, and describe our method for modeling the dynamic social network in Section 2.2. Then, in Section 2.3, we detail how we account for the fact that telemetry data are typically measured at individual-specific, irregularly spaced times with error.

2.1. *Position process.* A GMRF is a description of a Gaussian random vector where conditional dependence between elements is specified based on a neighborhood structure [Rue and Held (2005)]. For example, data occurring at regular intervals in time, or on a lattice in space, are often modeled with GMRFs because natural neighborhoods exist for each datum (e.g., the preceding measurement in time or the four closest spatial locations). Thus, GMRFs present a natural mathematical structure for modeling trajectories of connected individuals, as they provide a way to model dependence between connected or "neighboring" individuals.

We expect that social structure among individuals will influence their movement with respect to one another. Let $\boldsymbol{\mu}_i(t)$ denote the position of individual i at time t. Assuming we know the population social structure (i.e., which individuals are socially affiliated with which other individuals), we model the movements of all individuals simultaneously using a GMRF involving two social behavioral mechanisms: one related to attraction toward the mean position of connected individuals, and the other related to alignment or movement parallel to the paths taken by connected individuals. Although our model is flexible enough to capture attraction or repulsion, as well as alignment or anti-alignment, in most cases, we expect to infer assortative relations whereby individuals that are socially connected

move "together." For this reason, we discuss movement of connected individuals as aligned and attractive.

Attraction and alignment mechanisms are critical features of the mean positions of each individual at regular synchronous time steps. Models for locations on regular intervals have been developed by several others, including Brillinger and Stewart (1998), Jonsen, Flemming and Myers (2005), and Forester et al. (2007). We define the social relations in terms of a dynamic binary network $\mathbf{W}(t)$ indexed at times $t = 1, \ldots, T$, where entry $w_{ij}(t) = 1$ indicates a connection between individuals i and j at time t and $w_{ij}(t) = 0$ indicates a lack thereof.

We specify a GMRF conditionally from the perspective of a single individual at a given time. The mean position of each individual i at time t conditioned on all other individuals' positions at time t, denoted $\boldsymbol{\mu}_{-i}(t)$, and all positions at the previous time, $\boldsymbol{\mu}(t-1)$, follows a normal distribution with mean

$$\begin{aligned}&\mathbb{E}\big(\boldsymbol{\mu}_i(t)|\boldsymbol{\mu}_{-i}(t), \boldsymbol{\mu}(t-1), \mathbf{W}(t), \mathbf{W}(t-1), \alpha, \beta, \sigma^2, c\big)\\ &\quad\equiv \boldsymbol{\mu}_i(t-1)\\ &\qquad + \underbrace{\beta\tilde{\boldsymbol{\mu}}_i(t-1)}_{\text{attraction}} + \underbrace{\sum_{j\neq i}\alpha\frac{w_{ij}(t)}{w^c_{i+}(t)}\big(\boldsymbol{\mu}_j(t) - \big(\boldsymbol{\mu}_j(t-1) + \beta\tilde{\boldsymbol{\mu}}_j(t-1)\big)\big)}_{\text{alignment}}\end{aligned} \tag{1}$$

and precision

$$\operatorname{Prec}\big(\boldsymbol{\mu}_i(t)|\mathbf{W}(t), \sigma^2, c\big) \equiv \sigma^{-2} w^c_{i+}(t)\mathbf{I}_2. \tag{2}$$

Focusing on (1), we model the expected location of individual i as the sum of three terms: the individual's location in the previous time period, $\boldsymbol{\mu}_i(t-1)$; an attraction term capturing the tendency for the individual to move toward other individuals it is socially connected to; and an alignment term accounting for groups of interconnected individuals moving in the same general direction.

The term $\tilde{\boldsymbol{\mu}}_i(t)$ in the attraction component of (1) is a unit vector pointing from individual i's position $\boldsymbol{\mu}_i(t)$ to the mean position $\overline{\boldsymbol{\mu}}_i(t)$ of all the individuals it is connected to in $\mathbf{W}(t)$ (i.e., its ego-network):

$$\overline{\boldsymbol{\mu}}_i(t) \equiv \sum_{j\neq i}^{n} \frac{w_{ij}(t)}{w^c_{i+}(t)}\boldsymbol{\mu}_j(t), \tag{3}$$

$$\tilde{\boldsymbol{\mu}}_i(t) \equiv \begin{cases} \dfrac{\overline{\boldsymbol{\mu}}_i(t) - \boldsymbol{\mu}_i(t)}{\|\overline{\boldsymbol{\mu}}_i(t) - \boldsymbol{\mu}_i(t)\|_2}, & \displaystyle\sum_{j\neq i} w_{ij}(t) > 0,\\ 0, & \displaystyle\sum_{j\neq i} w_{ij}(t) = 0. \end{cases} \tag{4}$$

The parameter β controls the strength of the attractive effect of a social connection. On average, individual i moves a distance β in the direction $\tilde{\boldsymbol{\mu}}_i(t)$ during each time step.

In the above expression, $w_{i+}^{c}(t)$ is the size of individual i's ego-network at time t if the individual has at least one connection [i.e., $w_{i+}^{c}(t) = \sum_{j \neq i} w_{ij}(t)$], and equal to a constant $w_{i+}^{c}(t) = c > 0$ otherwise. We require c to be strictly positive so that the precision in (2) is nonzero for unconnected individuals.

The alignment term in (1) quantifies the mean displacement in position from $t-1$ to t for only those individuals that individual i is socially connected to, and after accounting for attraction. Although the sum is over all individuals j, the social network indicators $w_{ij}(t)$ eliminate the effects of an individual's direction if it is not connected to individual i. The parameter α controls the strength of the aligning effect, with 0 corresponding to no alignment and $\alpha \to 1$ corresponding to perfect alignment. The case $\alpha = 1$ corresponds to an intrinsic conditional autoregressive model with an improper covariance matrix. However, we limit our consideration to $\alpha < 1$, precluding this special case.

Finally, the expression for the precision in (2) has the property that individuals who are more socially connected [i.e., have larger ego-networks $w_{i+}^{c}(t)$] have larger precision. The proportional relationship between precision and $w_{i+}^{c}(t)$ is required for a valid GMRF, and aligns with our intuition that, conditioned on the position of all other individuals, the movement of an individual with few or no social connections is more difficult to predict than one that experiences strong attraction and alignment toward a large group of individuals. The parameter c can be thought of as the effective size of the ego-network for an unconnected individual with regard to precision.

The specification of the model in (1) and (2) properly defines a GMRF where the elements of the precision matrix at time t are

$$Q_{ij}(t) \equiv \begin{cases} -\alpha w_{ij}(t)\sigma^{-2}\mathbf{I}_2, & j \neq i, \\ w_{i+}^{c}(t)\sigma^{-2}\mathbf{I}_2, & j = i. \end{cases} \tag{5}$$

Therefore, we can write the multivariate version of the model for $t = 2, \ldots, T$ as

$$\left[\boldsymbol{\mu}_i(t) | \boldsymbol{\mu}_i(t-1), \boldsymbol{\theta}\right] \equiv \mathcal{N}\left(\boldsymbol{\mu}_i(t-1) + \beta\tilde{\boldsymbol{\mu}}_i(t-1), \mathbf{Q}(t)\right), \tag{6}$$

where we have concatenated the model parameters $(\alpha, \beta, p_1, \phi, \sigma^2, c, \mathbf{W})$ into a single vector $\boldsymbol{\theta}$ (note: p_1 and ϕ are parameters associated with the dynamic network $\mathbf{W}$ and are introduced in Section 2.2).

Notice that, for the joint distribution in (6), the attraction effect remains in the mean structure because the attraction force for an individual is toward the previous location of the individuals in the ego-network. However, the alignment effects are accounted for in the precision matrix because alignment is characterized by simultaneous movement of grouped individuals in the same direction. Figure 1 shows the alignment and attraction effects graphically.

The model for movement based on the normalized vector $\tilde{\boldsymbol{\mu}}_i(t)$, instead of $\overline{\boldsymbol{\mu}}_i(t) - \boldsymbol{\mu}_i(t)$, reflects a mechanistic understanding that attractive movement is often restricted by the distance an animal can reasonably travel in a given time

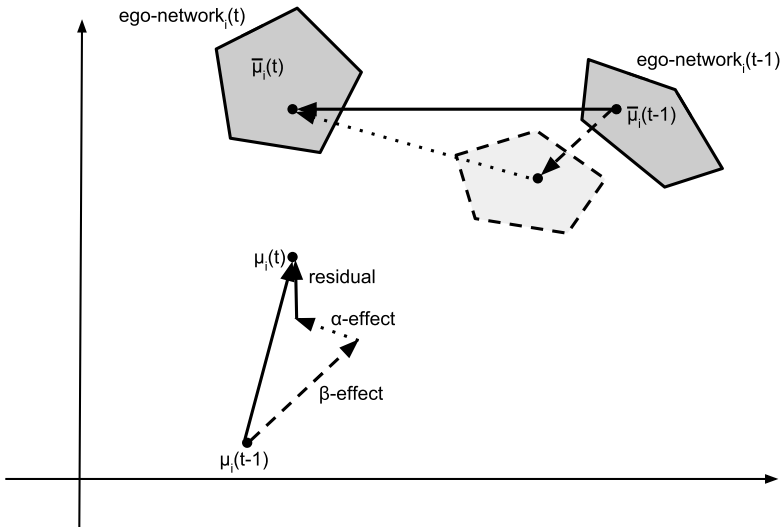

FIG. 1. *This schematic illustrates the two channels through which the dynamic social network influences movement. The dashed lines represent where the ego-network of individual i would be expected to be at time t under attraction alone, and the parallel dotted lines represent the alignment between individual i and the average of the differences* $\boldsymbol{\mu}_j(t) - (\boldsymbol{\mu}_j(t-1) + \beta\tilde{\boldsymbol{\mu}}_j(t-1))$.

step. We assume the maximum distance an individual is capable of moving during one time step to be approximately constant. Thus, when the gap between an individual and the center of its ego-network is large compared to its step size, an animal feeling an attractive pull will appear to take several steps of similar length in that direction.

If we had used the difference $\overline{\boldsymbol{\mu}}_i(t) - \boldsymbol{\mu}(t)$ instead of $\tilde{\boldsymbol{\mu}}(t)$ in the attraction component of (1), the attractive pull an individual experienced when its ego-network was far away could be far greater than the distance it was able to travel in a single time step. To see this, note that the interpretation of β in (6) would change to reflect the average proportion of the gap between an individual and the center of its ego-network covered during each time step. A value of $\beta = 0.5$ would imply that an animal closes half the distance between itself and the center of its ego-network, regardless of the size of that gap. In some cases, the proportional gap coverage model may be more appropriate. In our application with killer whales, it is reasonable for connections between animals to form across relatively large gaps in space relative to the distance an animal might be able to cover in a single time step. Thus, the former interpretation is the most appropriate for our application.

In (1) and (3) we define the vector $\overline{\boldsymbol{\mu}}_i(t-1)$ using the status of the social network at time $t-1$. Another possibility is to define $\overline{\boldsymbol{\mu}}_i(t-1)$ using the social

network at the current time t as

$$\overline{\boldsymbol{\mu}}_i(t-1) \equiv \sum_{j \neq i}^{n} \frac{w_{ij}(t)}{w_{i+}^{c}(t)} \boldsymbol{\mu}_j(t-1). \tag{7}$$

In practice, the differences that arise in the estimated social network depending on this modeling decision will only be noticeable near times when a connection status changes [i.e., whenever $\mathbf{w}(t) \neq \mathbf{w}(t-1)$]. Hence, when the estimated social network is slowly varying, like the one we observe in our application, we expect that these two definitions will result in essentially identical inference. However, for applications when the frequency of changes in social connections is high relative to the scale at which telemetry observations are made, the impact of the decision of how to define $\overline{\boldsymbol{\mu}}$ may be more significant.

2.2. *Dynamic social network.* We model the dynamic process that gives rise to $\mathbf{W}(t)$ as a collection of pairwise independent Bernoulli random variables with a Markovian dependence in time, where

$$w_{ij}(1) \sim \text{Bern}(p_1), \tag{8}$$

$$w_{ij}(t)|w_{ij}(t-1) \sim \begin{cases} \text{Bern}(p_{1|0}), & w_{ij}(t-1) = 0, \\ \text{Bern}(p_{1|1}), & w_{ij}(t-1) = 1, \end{cases} \qquad t = 2, \ldots, T. \tag{9}$$

The parameter p_1 is the probability of a social connection between any two individuals at time $t = 1$, $p_{1|0}$ is the conditional probability that a pair of individuals who are not connected at $t-1$ become connected at time t, and $p_{1|1}$ is the conditional probability that a pair connected at time $t-1$ remain connected at time t. Thus, our model for $\boldsymbol{\mu}$ can be thought of as a HMM where the latent social network $\mathbf{W}$ takes on the role of the hidden Markovian process. Though the model for the dynamic social network could be used exactly as specified in (8) and (9), we make two refinements that reduce the number of parameters we are required to estimate, and facilitate solicitation of priors.

First, we take advantage of the fact that, in many cases, it is reasonable to assume the mean density of a study population's dynamic social network remains constant in time. This is equivalent to requiring that the stationary distribution of the Markov process governing the overall network density match the expected density at time $t = 1$. Recall that we model the conditional distributions of the edges $\mathbf{w}(t)|\mathbf{w}(t-1)$ as independent Bernoulli random variables. Thus, the expected density of the network at time t is equal to the marginal probability of an edge between any two vertices, $\mathbb{P}(w_{ij}(t) = 1)$. The Markov process controlling network density is therefore the same as the process for the sequence of social connections $\mathbf{w}_{ij}$. Requiring that the initial density, p_1, match the stationary distribution of the Markov process is equivalent to the condition

$$p_1 = \frac{p_{1|0}}{p_{1|0} + 1 - p_{1|1}}. \tag{10}$$

Condition (10) implicitly reduces the number of parameters to be estimated from three to two.

The second refinement we make is a reparameterization that allows for more intuitive interpretation of model parameters, and hence facilitates the solicitation of priors. We define a new variable, ϕ, that controls the temporal stability of the dynamic network via

$$p_{1|0} \equiv (1-\phi)p_1, \tag{11}$$

which implies we can write $p_{1|1} = 1-(1-\phi)(1-p_1)$. As ϕ varies from 0 to 1, the social network transitions smoothly from complete temporal independence to complete temporal dependence (i.e., a static network where no edges form or dissolve in time). This can be expressed mathematically as $\lim_{\phi\to 0} p_{1|0} = \lim_{\phi\to 0} p_{1|1} = p_1$ and $\lim_{\phi\to 1}(1-p_{1|0}) = \lim_{\phi\to 1} p_{1|1} = 1$. Thus, ϕ can be thought of as a measure of the temporal range of dependence in the network. Under the parameterization using p_1 and ϕ, researchers can construct priors for the network density and stability independently of one another.

2.3. *Measurement error and time alignment.* Our model can be used to make inference about the posterior distribution of the model parameters $\boldsymbol{\theta}$ conditioned on the mean position process $\boldsymbol{\mu}$ (denoted $[\boldsymbol{\theta}|\boldsymbol{\mu}]$). However, in practice, we are rarely able to observe $\boldsymbol{\mu}$ directly. Rather, we observe noisy measurements of position at asynchronous, irregularly occurring times, which we denote $\mathbf{s}$, and the inference we wish to make is for the posterior distribution conditioned on observed data, not $\boldsymbol{\mu}$. Let $\mathbf{s}_i(\tau_i)$ denote the observed position of individual i at time τ_i, and $[\mathbf{s}|\boldsymbol{\mu}]$ the joint density of all observed locations conditioned on the unobserved processes $\boldsymbol{\mu}$. The top level of our hierarchical model provides a connection between the locations $\boldsymbol{\mu}_i(t)$, which occur at regular synchronized times, and the observations $\mathbf{s}_i(\tau_i)$.

We could obtain the desired posterior distribution by evaluating the integral

$$[\boldsymbol{\theta}|\mathbf{s}] = \int [\boldsymbol{\theta}|\boldsymbol{\mu}, \mathbf{s}][\boldsymbol{\mu}|\mathbf{s}]\, d\boldsymbol{\mu} \tag{12}$$

using Markov chain Monte Carlo (MCMC), provided we could sample from the distribution $[\boldsymbol{\mu}|\mathbf{s}]$. Unfortunately, because of the inherent complexities in the irregular, asynchronous observation times and the high dimensionality of the vector $\boldsymbol{\mu}$, sampling from this distribution becomes computationally infeasible when a study population contains more than a few individuals and a few dozen observation times per individual. We address this issue by making use of a multiple imputation procedure employed by Hooten et al. (2010) and Hanks et al. (2015, 2011), paired with a continuous-time correlated random walk model from Johnson et al. (2008). Multiple imputation offers a computationally efficient way to account for asynchronous, noisy position measurements while still permitting us to use a discrete-time, step-aligned structure for movement informed by a dynamic social network. We outline

the procedure briefly below, and refer the reader to Hooten et al. (2010) and Hanks et al. (2011) for further details.

The premise of the multiple imputation strategy assumes the existence of a distribution that is very similar to $[\boldsymbol{\mu}|\mathbf{s}]$ from which we can sample paths easily. If we can define such a distribution, which we call $[\boldsymbol{\mu}^*|\mathbf{s}]$, then we can closely approximate the integral in (12) by

$$[\boldsymbol{\theta}|\mathbf{s}] \approx \int [\boldsymbol{\theta}|\boldsymbol{\mu} = \boldsymbol{\mu}^*][\boldsymbol{\mu}^*|\mathbf{s}]\, d\boldsymbol{\mu}^*. \tag{13}$$

We can evaluate the integral in (13) up to a constant of proportionality by drawing a realization from $[\boldsymbol{\mu}^*|\mathbf{s}]$ at every iteration of our MCMC algorithm and updating model parameters $\boldsymbol{\theta}$ conditioned on the realization.

Johnson et al. (2008) introduced a continuous-time correlated random walk model for movement with measurement error that relies on an Ornstein–Uhlenbeck process for velocity and treats the observed paths for each individual as conditionally independent (i.e., $[\mathbf{s}_i|\boldsymbol{\mu}^*] = [\mathbf{s}_i|\boldsymbol{\mu}_i^*]$). Continuing with the same model, Johnson, London and Kuhn (2011) provided an approach for sampling from the posterior predictive path, $[\boldsymbol{\mu}_i^*|\mathbf{s}_i]$, which we use to evaluate the integral in (13).

We approximate the desired posterior using the following two-step procedure:

1. Draw K different realizations from $[\boldsymbol{\mu}^*|\mathbf{s}]$ using the `R` package `crawl` [Johnson et al. (2008)].
2. At each iteration of the MCMC sampler, draw one of the K samples and condition on $\boldsymbol{\mu}^*$ for parameter updates.

Choosing too small a value for K will result in inference for the social network that does not properly account for the uncertainty in $\boldsymbol{\mu}$ arising due to measurement error and temporal asynchronicity, and can potentially be biased depending on the particular draws from $[\boldsymbol{\mu}^*|\mathbf{s}]$. In practice, we found a sufficiently large K in our application to be on the order of 50, as parameter estimates were essentially unchanged for larger K. By making use of the two-stage sequential procedure, we are fitting a close approximation to the full Bayesian hierarchical model.

2.4. *Priors*. To demonstrate the value of our model when little is known a priori about the social ties in a study population, we specify diffuse priors for most parameters in both the simulation and application. We select conjugate parametric families whenever possible. The priors used in our simulation and application are shown in the right columns of Tables 1 and 2. While more informative priors could be used when expert knowledge is available, we found most parameters to be insensitive to the choice of hyperparameters. The one exception is the network stability parameter ϕ (see Section 2.2). The stability of the network determines the range of temporal dependence in the dynamic social network. Similar to analogous range parameters in the geostatistical setting [see, for example, Chapter 6 of Gelfand et al. (2010)], ϕ can prove difficult to estimate from the data. In our

TABLE 1
Marginal posterior medians and 95% credible intervals for model parameters. True values for the simulation were chosen to yield plausible movement paths. The right column describes the prior distributions used

		Posterior		Prior
Parameter	**True**	**Median**	**(2.5%, 97.5%)**	**Density**
α	0.9	0.92	(0.77, 0.96)	Unif$(-1, 1)$
β	0.5	0.46	(0.37, 0.55)	$\mathcal{N}(0, 10^3)$
p_1	0.2	0.15	(0.0096, 0.21)	Unif$(0, 1)$
ϕ	0.95	0.84	(0.78, 0.90)	Beta$(17.2, 1.5)$
c	0.33	0.30	(0.24, 2.36)	IG$(1.5, 3.5)$
σ^2	1	0.92	(0.74, 7.91)	IG$(10^{-1}, 10^{-3})$

application (Section 4), we used an informative prior that implies a strongly stable network because we expected the social network to change slowly relative to the time scale at which the telemetry data were gathered.

3. Simulation. The primary parameters of scientific interest are in the network $\mathbf{W}$. Thus, we evaluate the quality of our model by assessing its ability to recover the network. A baseline model for comparison is one using only proximity as a criterion for social connectivity. We consider the proximity-based network defined by

$$W_{ij}^R(t) = I_{\|\boldsymbol{\mu}_i - \boldsymbol{\mu}_j\|_2 < R}. \tag{14}$$

Though it does not explicitly incorporate the behaviors of attraction and alignment, defining the network using (14) is computationally cheap and closely mirrors the

TABLE 2
Marginal posterior medians and 95% credible intervals for model parameters when fit to the killer whale tagging data. The values reflect a strong alignment effect (α), weak attraction effect (β) and a stable (ϕ), sparse (p_1) social network. The right column describes the prior distributions used

	Posterior		Prior
Parameter	**Median**	**(2.5%, 97.5%)**	**Density**
α	0.88	(0.40, 0.94)	Unif$(-1, 1)$
β	0.022	(0.012, 0.030)	$\mathcal{N}(0, 10^3)$
p_1	0.11	(0.005, 0.20)	Unif$(0, 1)$
ϕ	0.95	(0.90, 0.98)	Beta$(100, \frac{100}{9})$
c	0.35	(0.24, 2.87)	IG$(1.5, 3.5)$
σ	0.0033	(0.0026, 0.025)	IG$(10^{-1}, 10^{-3})$

way some data are collected in the field [Goldenberg et al. (2014), Levin et al. (2015)]. The proximity-based approach therefore represents a viable alternative against which we can compare our model. However, failing to consider attraction and alignment effects, as well as temporal stability in a dynamic social network, can lead to spurious associations that arise when two unconnected individuals happen to pass each other by chance. Our simulation shows that our model is able to avoid such pitfalls.

In the following simulation, we generate directly from the proposed process model and fit the model using paths $\boldsymbol{\mu}$. We use parameter values (shown in Table 1) that generate paths closely resembling the data in our application for killer whales. Details of the methods we used to fit the model may be found in Supplement A [Scharf et al. (2016a)], and the `R` code used to produce this simulation study is provided in Supplement C [Scharf et al. (2016c)]. We used the posterior mean of $\mathbf{W}$ as a summary of the network, and investigated a variety of radii R with the proximity-based network, $\mathbf{W}^R$, to define a suite of alternatives. Because we know the true mean density of the network, p_1, we select the proximity-based network for which the radius yields a mean density as close as possible to the true value. Choosing a radius that recovers the true mean density would not generally be possible, thus, we compared our model to a particularly favorable proximity-based alternative. However, we found that proximity alone provides a poor estimate of the true network relative to our proposed dynamic network model.

Figure 2 shows estimates of $\mathbf{W}$ for a random selection of pairs. Included on each plot are the true network (dashed), the posterior mean from the model fit (solid) and the proximity-based estimate (dotted). Although the posterior mode of $w_{ij}(t)$ would be a natural choice for a prediction of the true dynamic social network, we plot the posterior mean because it provides a visual description about uncertainty in our predicted network. For example, posterior means of $w_{ij}(t)$ near 0.5 indicate larger uncertainty about the true connection status of individuals i and j at time t than posterior means near 0 or 1. The pairs 1–5 (top left) and 1–6 (bottom right) show how the proximity-based network can both find spurious connections and fail to identify connected behavior when it takes place over too large a distance. Table 1 shows 95% credible intervals for all parameters in the model except $\mathbf{W}$. All credible intervals capture the true parameter values, except those for ϕ. We observed moderate systematic bias in the posterior distribution of ϕ toward zero, however, posterior inferences for $\mathbf{W}$ were robust despite the bias in ϕ. In most applications we expect that the primary questions of scientific interest concern the network $\mathbf{W}$, and ϕ can be treated as a nuisance parameter.

Any study of a social network is ultimately based on a definition for connection specific to the population of interest. Thus, it is incorrect to say that the proximity-based network fails to capture the true network. Rather, the proximity-based network simply does a poorer job describing the connections that influence movement than the network based on our proposed model. It is impossible to perfectly define a given social network, but if there is reason to believe that a study population

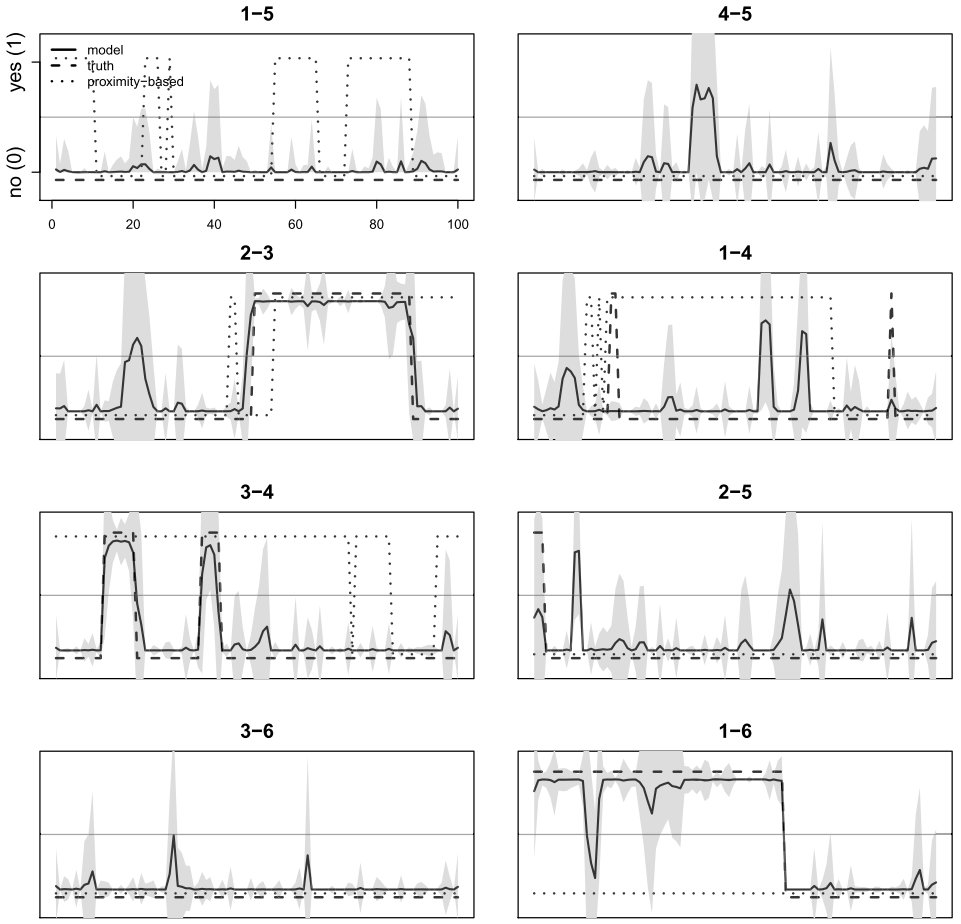

FIG. 2. *A subset of the complete estimated dynamic network for the simulated data on six individuals. The titles correspond to the* i*th and* j*th individuals in* $w_{ij}(t)$*. The dashed line is the true network, the solid line is the posterior mean from the proposed Bayesian model, and the gray region represents one standard deviation above and below the posterior mean. The dotted line shows the network defined by* $\mathbf{W}^R$*, where individuals are deemed connected whenever they are separated by a distance less than* R *(see Section 3). (Note: The lines are offset slightly near* 0 *and* 1 *for visual clarity.)*

might exhibit the commonly observed behaviors of attraction and alignment, then our model offers a way to study it. We have shown that ignoring these mechanisms can result in misleading inference.

4. Killer whales. We analyzed observed data for seven individuals near the Antarctic Peninsula over the course of a week in February 2013 [for a description of the tags and study area see Andrews, Pitman and Ballance (2008), Durban and Pitman (2012)]. Geographic positions were measured using Argos transmitter tags.

Within the study area, three genetically distinct types of killer whales (termed A, B1 and B2) are known to exist [Durban et al. (2016), Morin et al. (2015), Pitman and Ensor (2003)] and are characterized primarily by their size, coloration and diet. Type A killer whales are the largest and feed primarily on Antarctic minke whales (*Balaenoptera bonaerensis*) [Pitman and Ensor (2003)]. Of the two type B killer whales, B1 is larger and is distinguished by a diet consisting primarily of ice seals [Durban and Pitman (2012)]. Finally, type B2 killer whales are distinguished by an observed diet of penguins and likely also fish during deep dives [Durban et al. (2016), Pitman and Durban (2010)]. Although all types of killer whales have been observed exhibiting social behavior within type, association between types has not been observed. The study sample of seven tagged whales consisted of three whales of Type A, one of type B1 and three of type B2.

Credible intervals for all parameters except the network $\mathbf{W}$ are shown in Table 2. When we examine the mean step size across all individuals and times, we found it to be several times larger than the contribution of attraction, suggesting only a moderate attractive effect. The fit also suggests a strong alignment effect evidenced by the posterior median for α near 1. Therefore, we conclude that connectivity in this population of killer whales manifests itself predominantly as movement in parallel, with some additional tendency for connected individuals to move toward one another.

The credible intervals for p_1 and ϕ suggest that the network is very stable, but also fairly sparse. Enduring connections are directly visible in Figure 3. The left column shows all pairwise dynamics between the three individuals of type B2, and the right column shows all pairwise dynamics between the three individuals of type A. All three individuals of type B2 show strong connection through the study period and, in fact, all three of these individuals moved as a group during this time. The only social interaction involving individuals in type A occurred during the first few days of the study period between individuals 5 and 6. There was strong evidence for complete independence between all individuals not in the same type (see Figures 4 and 5 in the Supplement [Scharf et al. (2016a, 2016b, 2016c)]), consistent with expert knowledge. Of the 15 inter-type connections in $\mathbf{W}$, there were no posterior means above 0.5 at any time in the study period. A visualization of the movement and estimated social connections between these individuals can be found in Supplement B [Scharf et al. (2016b)].

As in the simulation (Section 3), we investigated an alternative definition for the social network, based purely on proximity, given by (14). To account for the uncertainty in $\boldsymbol{\mu}$, we constructed the proximity-based network, defined by a particular choice of R for each of the K draws from $[\boldsymbol{\mu}^*|\mathbf{s}]$ used for multiple imputation (see Section 2.3), and averaged across these networks. The primary means of communication at a distance between killer whales is acoustic signaling. Therefore, we selected values for R based on the typical distances across which killer whales are known to communicate acoustically. Miller (2006) observed killer whales in the Pacific Northwest and estimated signals between individuals were detectable

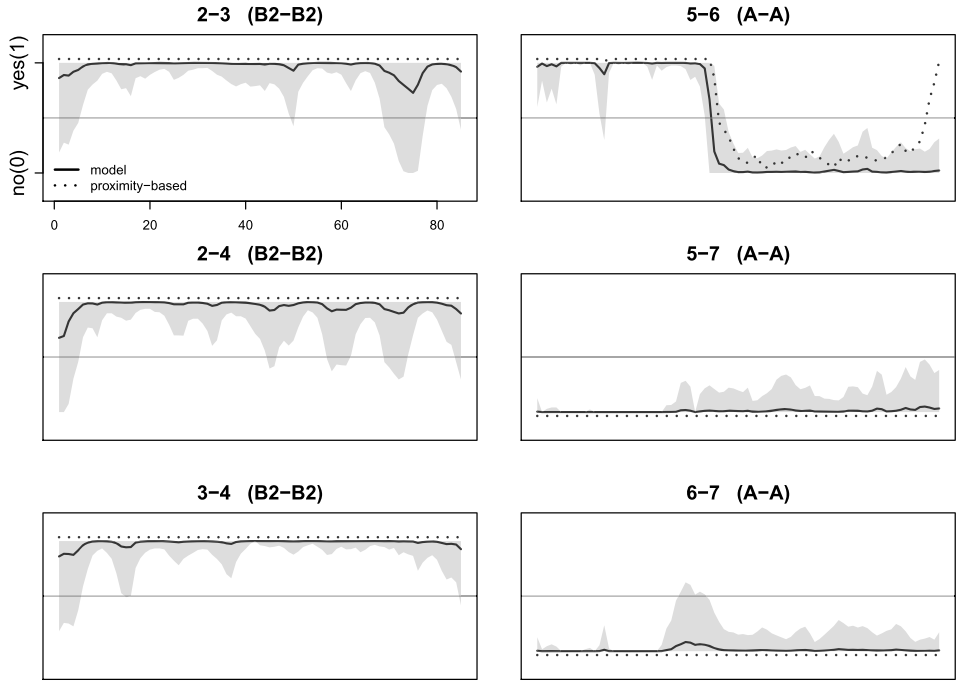

FIG. 3. *A selection of the* $\binom{7}{2} = 21$ *possible pairs of individuals in the killer whale study sample. The left column is all pairs of killer whales of type B*2 (*labeled* 2, 3, 4), *and the right column is all pairs of killer whales of type A* (*labeled* 5, 6, 7). *The solid line in each plot shows the posterior mean for* w_{ij} *and the gray region represents one standard deviation above and below the posterior mean. The dotted line shows the network defined by* $\mathbf{W}^R$, *where individuals are deemed connected whenever they are separated by a distance less than* R. (*Note*: *The lines are offset slightly near* 0 *and* 1 *for visual clarity.*)

at distances of 5–15 km. This range is consistent with expert knowledge about the killer whales in our study region. We inspected the corresponding dynamic social networks for radii between 5–15 km and found little variation in the resulting networks. Figures 3, 4 and 5 show the proximity-based network for $R = 10$ km.

While we observed some similarities in the proximity-based and model-based networks, there are several notable discrepancies. For instance, all proximity-based networks for radii between 5–15 km included numerous connections between individuals of different types (Figures 4 and 5). The presence of inter-type connections conflicts with expert knowledge that killer whales of differing types do not form social bonds, suggesting that the proximity-based network may be defining spurious social ties. Moreover, because the proximity-based network does not account for temporal stability in social connections, we observe instances of implausibly rapid oscillation in connection status (Figure 5). The proximity-based networks and our model-based network provide similar inference for within-type ties (Figure 3), but our model-based approach also provides rigorous uncertainty estimates.

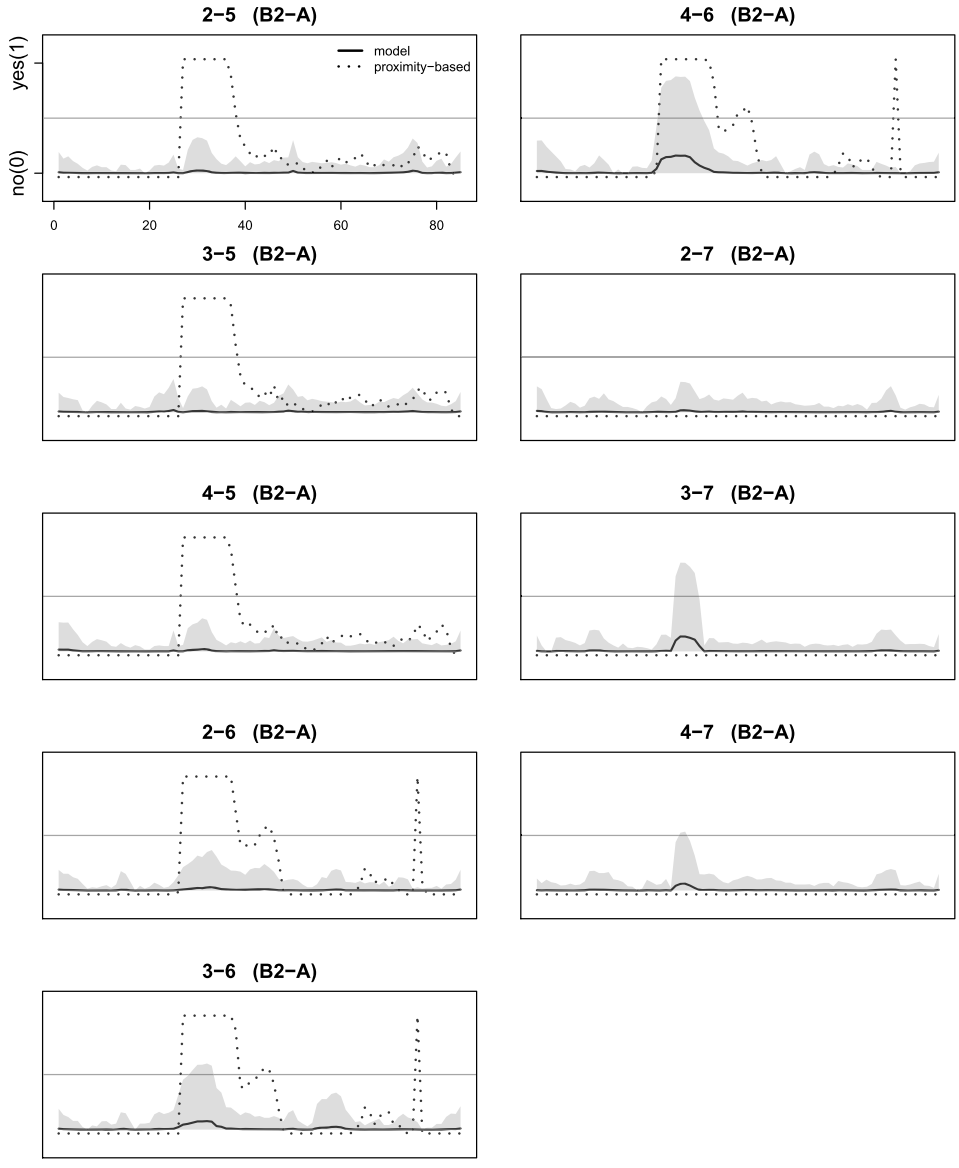

FIG. 4. *A selection of the* $\binom{7}{2} = 21$ *possible pairs of individuals in the killer whale study sample. The plots displayed are for all inter-type pairs of killer whales of type B*2 (*labeled* 2, 3, 4) *and A* (*labeled* 5, 6, 7). *The solid line in each plot shows the posterior mean for* w_{ij} *and the gray region represents one standard deviation above and below the posterior mean. The dotted line shows the network defined by* $\mathbf{W}^R$, *where individuals are deemed connected whenever they are separated by a distance less than* R. *No posterior means above* 0.5 *were predicted for inter-type connections*. (*Note*: *The lines are offset slightly near* 0 *and* 1 *for visual clarity.*)

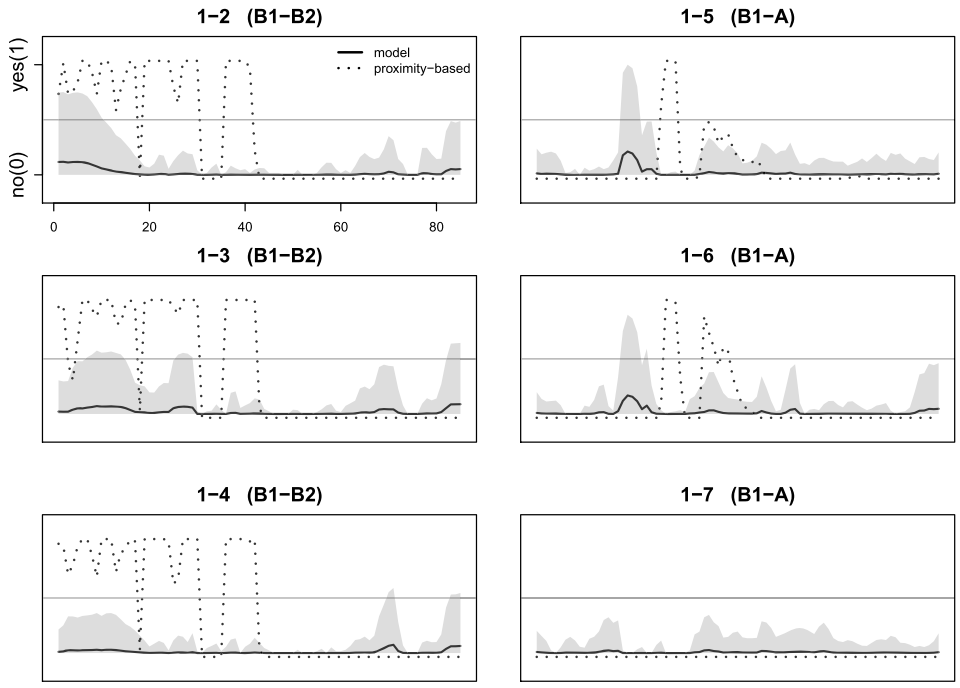

FIG. 5. *A selection of the* $\binom{7}{2} = 21$ *possible pairs of individuals in the killer whale study sample. The plots displayed are for all inter-type pairs of killer whales between the sole individual of type B*1 (*labeled* 1) *and those of type B*2 (*labeled* 2, 3, 4) *and A* (*labeled* 5, 6, 7). *The solid line in each plot shows the posterior mean for* w_{ij} *and the gray region represents one standard deviation above and below the posterior mean. The dotted line shows the network defined by* $\mathbf{W}^R$, *where individuals are deemed connected whenever they are separated by a distance less than R. No posterior means above* 0.5 *were predicted for inter-type connections.* (*Note*: *The lines are offset slightly near* 0 *and* 1 *for visual clarity.*)

A researcher might arguably make an *ad hoc* adjustment to the proximity-based network and simply discard all inter-type connections on the basis of prior knowledge, thereby arriving at the same conclusion regardless of which rule was used to define the social network. However, the feasibility of such an approach is unique to this study for two reasons. First, supplementary individual-level information, such as killer whale type, is often unavailable. Second, in many populations, the relationship among covariates and social connections is largely unknown, prohibiting covariate-based pruning of the proximity network.

5. Discussion. Existing methods for measuring and studying dynamic social networks in animal populations typically involve *ad hoc* definitions for connectivity based on direct observation of study populations. Our model offers a flexible, but interpretable, hierarchical framework that allows researchers to rigorously study dynamic social networks informed by relatively inexpensive telemetry data.

Moreover, our proposed model can easily be coupled with existing analyses on dynamic networks. Fundamentally, the study of dynamic social networks often begins with descriptive statistics such as network density, node degree, transitivity and others [Pinter-Wollman et al. (2013)]. All of these common summaries can be obtained as derived quantities in our Bayesian framework with estimates of uncertainty. More sophisticated models for dynamic networks [e.g., Durante and Dunson (2014), Sarkar and Moore (2005), Sewell and Chen (2015)] can take the posterior mode of $\mathbf{W}$ as input or be incorporated as part of a larger hierarchical modeling structure.

We have shown, through simulation, that our proposed model is able to capture information about a population's social structure in a way that a simplistic proximity-based measure cannot, both by avoiding spurious connections and detecting interactions that occur over large distances. Through an application on killer whale movement, we showed that the model captures connections consistent with expert knowledge based on nonquantitative observation, and can therefore be relied upon to deliver credible and practical inference.

When auxiliary covariates are available on the individuals, the proposed model can be extended to include such data. A potential generalization is to allow the spatial covariates to influence the mean position process of each individual, $\boldsymbol{\mu}_i(t)$, linearly. If we denote the matrix containing spatial covariates $\mathbf{X}_C(t)$, we arrive at a familiar additive form

$$[\boldsymbol{\mu}(t)|\boldsymbol{\mu}(t-1),\boldsymbol{\theta},\boldsymbol{\gamma}] = \mathcal{N}(\underbrace{\mathbf{X}_C(t-1)\boldsymbol{\gamma}}_{\text{covariate effect}} + \underbrace{\mathbf{X}_W(t-1)\boldsymbol{\beta}}_{\text{attraction}}, \underbrace{\mathbf{Q}(t)}_{\text{alignment}}), \tag{15}$$

where

$$\mathbf{X}_W(t-1) \equiv [\boldsymbol{\mu}(t-1) \quad \tilde{\boldsymbol{\mu}}(t-1)], \qquad \boldsymbol{\beta} \equiv \begin{bmatrix} 1 \\ \beta \end{bmatrix}. \tag{16}$$

One limitation of our model is that it is computationally intensive for large study samples. The number of parameters in our model grows at a rate of $\binom{n}{2}T$ as the number of individuals, n, and number of time points, T, increase. The most dominant factor in computation time is typically n, and when the number of individuals grows beyond a few dozen, fitting the model on a laptop computer using MCMC becomes infeasible. One way to decrease the computational cost of fitting the model is to introduce additional structure on $\mathbf{W}$. We suggest two possible approaches.

The first way to introduce structure to $\mathbf{W}$ is to define a maximum radius of interaction, $R_{\max}$, beyond which the probability of a social connection is zero. For example, the radius might be chosen to be the maximum distance at which two individuals are able to detect one another. After modifying the conditional distribution of $w_{ij}(t)$ based on $R_{\max}$, it is no longer necessary to update all $w_{ij}(t)$ in each step of the MCMC algorithm, only those for which $\|\boldsymbol{\mu}_i(t) - \boldsymbol{\mu}_j(t)\| < R_{\max}$. If $R_{\max}$ is small relative to the spatial extent of the trajectories, this proximity-based

modification offers a substantial reduction in the computational cost of fitting the model. This idea is somewhat related to covariance tapering for spatially referenced Gaussian random variables. Furrer, Genton and Nychka (2006) decrease the computational burden of interpolating, or kriging, by deliberately introducing zeros into the covariance matrix. In our setting, we would introduce zeros into the precision matrix.

Another way to alleviate the computational burden is to enforce structure directly on $\mathbf{W}$ to reduce the number of parameters in the model. For instance, it may be reasonable to assume that the social connections in a given population form as complete subgroups or cliques. In this case, the network describes a clustering process with only nT parameters. Though motivated by straightforward mechanisms, both of these approaches to reducing the computational burden are nontrivial to implement. In the first case, setting a maximum radius of interaction complicates the enforcement of stability in the density of the network (introduced in Section 2.2) and offers modest or no gains when $R_{\max}$ is large relative to the spatial extent of the individual paths. In the second case, updating the clustering process $\mathbf{W}$ requires the exploration of a very large space (of cardinality equal to the Bell number B_n) for every t.

Although further developments are required before data for large populations of individuals can be accommodated, our framework provides a strong foundation for modeling relationships between movement and social networks.

Acknowledgments. Killer whale tagging was conducted under permit #14097 from the National Marine Fisheries Service and Antarctic Conservation Act permit #2009-013. Shipboard tagging operations were supported by Lindblad Expeditions and the National Geographic Society, and by an NSF rapid grant to Ari Friedlaender. Robert Pitman helped with tag deployments and identification of killer whale types in the field.

Any use of trade, firm or product names is for descriptive purposes only and does not imply endorsement by the U.S. Government.

We would like to thank multiple anonymous reviewers for providing valuable feedback on this manuscript.

SUPPLEMENTARY MATERIAL

Supplement A: MCMC details (DOI: 10.1214/16-AOAS970SUPPA; .zip). Priors and full-conditionals for the model are presented.

Supplement B: Animation (DOI: 10.1214/16-AOAS970SUPPB; .zip). Animation of killer whales.

Supplement C: R code (DOI: 10.1214/16-AOAS970SUPPC; .zip). Code used for simulation in Section 3.

REFERENCES

ANDREWS, R. D., PITMAN, R. L. and BALLANCE, L. T. (2008). Satellite tracking reveals distinct movement patterns for type B and type C killer whales in the southern Ross sea, Antarctica. *Polar Biol*. **31** 1461–1468.

BAIRD, R. W. and WHITEHEAD, H. (2000). Social organization of mammal-eating killer whales: Group stability and dispersal patterns. *Can. J. Zool*. **78** 2096–2105.

BERLINER, L. M. (1996). Hierarchical Bayesian time series models. In *Maximum Entropy and Bayesian Methods* (*Santa Fe*, *NM*, 1995) (K. M. Hanson and R. N. Silver, eds.). *Fund. Theories Phys*. **79** 15–22. Kluwer Academic, Dordrecht. MR1446713

BESAG, J. (1974). Spatial interaction and the statistical analysis of lattice systems. *J. Roy. Statist. Soc. Ser. B* **36** 192–236. MR0373208

BESAG, J. and KOOPERBERG, C. (1995). On conditional and intrinsic autoregressions. *Biometrika* **82** 733–746. MR1380811

BRILLINGER, D. R. and STEWART, B. S. (1998). Elephant-seal movements: Modelling migration. *Canad. J. Statist*. **26** 431–443.

CODLING, E. A. and BODE, N. W. (2014). Copycat dynamics in leaderless animal group navigation. *Movement Ecology* **2** 11.

CROFT, D. P., JAMES, R. and KRAUSE, J. (2008). *Exploring Animal Social Networks*. Princeton Univ. Press, Princeton, NJ.

DURANTE, D. and DUNSON, D. B. (2014). Nonparametric Bayes dynamic modelling of relational data. *Biometrika* **101** 883–898. MR3286923

DURBAN, J. W. and PITMAN, R. L. (2012). Antarctic killer whales make rapid, round-trip movements to subtropical waters: Evidence for physiological maintenance migrations? *Biol. Lett*. **8** 274–277.

DURBAN, J. W., FEARNBACH, H., BURROWS, D. G., YLITALO, G. M. and PITMAN, R. L. (2016). morphological and ecological evidence for two sympatric forms of Type B killer whale around the Antarctic peninsula. *Polar Biology* **April** 1–6.

FORESTER, J. D., IVES, A. R., TURNER, M. G., ANDERSON, D. P., FORTIN, D., BEYER, H. L., SMITH, D. W. and BOYCE, M. S. (2007). State-space models link elk movement patterns to landscape characteristics in Yellowstone National Park. *Ecol. Mono*. **77** 285–299.

FRANZ, M., MCLEAN, E., TUNG, J., ALTMANN, J. and ALBERTS, S. C. (2015). Self-organizing dominance hierarchies in a wild primate population. *Proceedings of the Royal Society B*: *Biological Sciences* **282** 20151512.

FURRER, R., GENTON, M. G. and NYCHKA, D. (2006). Covariance tapering for interpolation of large spatial datasets. *J. Comput. Graph. Statist*. **15** 502–523. MR2291261

GELFAND, A. E., DIGGLE, P., GUTTORP, P. and FUENTES, M. (2010). *Handbook of Spatial Statistics*, CRC Press, Boca Raton, FL.

GOLDENBERG, S. Z., DE SILVA, S., RASMUSSEN, H. B., DOUGLAS-HAMILTON, I. and WITTEMYER, G. (2014). Controlling for behavioural state reveals social dynamics among male African elephants, *Loxodonta africana*. *Anim. Behav.* **95** 111–119.

HANKS, E. M., HOOTEN, M. B., JOHNSON, D. S. and STERLING, J. T. (2011). Velocity-based movement modeling for individual and population level inference. *PLoS ONE* **6** e22795.

HANKS, E. M., SCHLIEP, E. M., HOOTEN, M. B. and HOETING, J. A. (2015). Restricted spatial regression in practice: Geostatistical models, confounding, and robustness under model misspecification. *Environmetrics* **26** 243–254. MR3340961

HOOTEN, M. B., JOHNSON, D. S., HANKS, E. M. and LOWRY, J. H. (2010). Agent-based inference for animal movement and selection. *J. Agric. Biol. Environ. Stat*. **15** 523–538. MR2788638

JOHNSON, D. S., LONDON, J. M. and KUHN, C. E. (2011). Bayesian inference for animal space use and other movement metrics. *J. Agric. Biol. Environ. Stat*. **16** 357–370. MR2843131

JOHNSON, D. S., LONDON, J. M., LEA, M.-A. and DURBAN, J. W. (2008). Continuous-time correlated random walk model for animal telemetry data. *Ecology* **89** 1208–1215.

JONSEN, I. D., FLEMMING, J. M. and MYERS, R. A. (2005). Robust state-space modeling of animal movement data. *Ecology* **86** 2874–2880.

KRAUSE, J., CROFT, D. P. and JAMES, R. (2007). Social network theory in the behavioural sciences: Potential applications. *Behav. Ecol. Sociobiol.* **62** 15–27.

LANGROCK, R., KING, R., MATTHIOPOULOS, J., THOMAS, L., FORTIN, D. and MORALES, J. M. (2012). Flexible and practical modeling of animal telemetry data: Hidden Markov models and extensions. *Ecology* **93** 2336–2342.

LANGROCK, R., HOPCRAFT, J. G. C., BLACKWELL, P. G., GOODALL, V., KING, R., NIU, M., PATTERSON, T. A., PEDERSEN, M. W., SKARIN, A. and SCHICK, R. S. (2014). Modelling group dynamic animal movement. *Methods in Ecology and Evolution* **5** 190–199.

LEMASSON, B. H., ANDERSON, J. J. and GOODWIN, R. A. (2013). Motion-guided attention promotes adaptive communications during social navigation. *Proceedings of the Royal Society B*: *Biological Sciences* **280** 20122003.

LEVIN, I. I., ZONANA, D. M., BURT, J. M. and SAFRAN, R. J. (2015). Performance of encounternet tags: Field tests of miniaturized proximity loggers for use on small birds. *PLoS ONE* **10** e0137242.

MCCLINTOCK, B. T., JOHNSON, D. S., HOOTEN, M. B., HOEF, J. M. V. and MORALES, J. M. (2014). When to be discrete: The importance of time formulation in understanding animal movement. *Movement Ecology* **2** 21.

MILLER, P. J. O. (2006). Diversity in sound pressure levels and estimated active space of resident killer whale vocalizations. *J. Comp. Physiol. A Neuroethol. Sens. Neural. Behav. Physiol.* **192** 449–459.

MORALES, J. M., MOORCROFT, P. R., MATTHIOPOULOS, J., FRAIR, J. L., KIE, J. G., POWELL, R. A., MERRILL, E. H. and HAYDON, D. T. (2010). Building the bridge between animal movement and population dynamics. *Philosophical Transactions of the Royal Society B*: *Biological Sciences* **365** 2289–2301.

MORIN, P. A., PARSONS, K. M., ARCHER, F. I., ÁVILA-ARCOS, M. C., BARRETT-LENNARD, L. G., DALLA ROSA, L., DUCHÊNE, S., DURBAN, J. W., ELLIS, G. M., FERGUSON, S. H., FORD, J. K., FORD, M. J., GARILAO, C., GILBERT, M. T. P., KASCHNER, K., MATKIN, C. O., PETERSEN, S. D., ROBERTSON, K. M., VISSER, I. N., WADE, P. R., HO, S. Y. W. and FOOTE, A. D. (2015). geographical and temporal dynamics of a global radiation and diversification in the killer whale. *Mol. Ecol.* **24** 3964–3979.

PARSONS, K. M., BALCOMB, K. C., FORD, J. K. B. and DURBAN, J. W. (2009). The social dynamics of southern resident killer whales and conservation implications for this endangered population. *Anim. Behav.* **77** 963–971.

PINTER-WOLLMAN, N., HOBSON, E. A., SMITH, J. E., EDELMAN, A. J., SHIZUKA, D., DE SILVA, S., WATERS, J. S., PRAGER, S. D., SASAKI, T., WITTEMYER, G., FEWELL, J. and MCDONALD, D. B. (2013). The dynamics of animal social networks: Analytical, conceptual, and theoretical advances. *Behavioral Ecology* art047.

PITMAN, R. L. and DURBAN, J. W. (2010). Killer whale predation on penguins in Antarctica. *Polar Biol.* **33** 1589–1594.

PITMAN, R. L. and DURBAN, J. W. (2012). Cooperative hunting behavior, prey selectivity and prey handling by pack ice killer whales (*Orcinus orca*), type B, in Antarctic Peninsula waters. *Mar. Mamm. Sci.* **28** 16–36.

PITMAN, R. L. and ENSOR, P. (2003). Three forms of killer whales (*Orcinus orca*) in Antarctic waters. *J. Cetacean Res. Manag.* **5** 131–140.

RUE, H. and HELD, L. (2005). *Gaussian Markov Random Fields*: *Theory and Applications*. *Monographs on Statistics and Applied Probability* **104**. Chapman & Hall, Boca Raton, FL. MR2130347

RUSSELL, J. C., HANKS, E. M. and HARAN, M. (2015). Dynamic models of animal movement with spatial point process interactions. *J. Agric. Biol. Environ. Stat.* 1–19.

SARKAR, P. and MOORE, A. W. (2005). Dynamic social network analysis using latent space models. *ACM SIGKDD Explor. Newsl.* **7** 31–40.

SCHARF, H. R., HOOTEN, M. B., FOSDICK, B. K., JOHNSON, D. S., LONDON, J. M. and DURBAN, J. W. (2016a). Supplement to "Dynamic social networks based on movement." DOI:10.1214/16-AOAS970SUPPA.

SCHARF, H. R., HOOTEN, M. B., FOSDICK, B. K., JOHNSON, D. S., LONDON, J. M. and DURBAN, J. W. (2016b). Supplement to "Dynamic social networks based on movement." DOI:10.1214/16-AOAS970SUPPB.

SCHARF, H. R., HOOTEN, M. B., FOSDICK, B. K., JOHNSON, D. S., LONDON, J. M. and DURBAN, J. W. (2016c). Supplement to "Dynamic social networks based on movement." DOI:10.1214/16-AOAS970SUPPC.

SEWELL, D. K. and CHEN, Y. (2015). Latent space models for dynamic networks. *J. Amer. Statist. Assoc.* **110** 1646–1657. MR3449061

SIH, A., HANSER, S. F. and MCHUGH, K. A. (2009). Social network theory: New insights and issues for behavioral ecologists. *Behav. Ecol. Sociobiol.* **63** 975–988.

WEY, T., BLUMSTEIN, D. T., SHEN, W. and JORDÁN, F. (2008). Social network analysis of animal behaviour: A promising tool for the study of sociality. *Anim. Behav.* **75** 333–344.

WILLIAMS, R. and LUSSEAU, D. (2006). A killer whale social network is vulnerable to targeted removals. *Biol. Lett.* **2** 497–500.

WILLIAMS, R., TRITES, A. W. and BAIN, D. E. (2002). Behavioural responses of killer whales (*Orcinus orca*) to whale-watching boats: Opportunistic observations and experimental approaches. *J. Zool.* **256** 255–270.

H. R. SCHARF
B. K. FOSDICK
DEPARTMENT OF STATISTICS
COLORADO STATE UNIVERSITY
FORT COLLINS, COLORADO 80523
USA
E-MAIL: henry.scharf@colostate.edu
bailey.fosdick@colostate.edu

M. B. HOOTEN
U.S. GEOLOGICAL SURVEY
COLORADO COOPERATIVE FISH
AND WILDLIFE RESEARCH UNIT
DEPARTMENT OF FISH, WILDLIFE,
AND CONSERVATION BIOLOGY
AND
DEPARTMENT OF STATISTICS
COLORADO STATE UNIVERSITY
201 JVK WAGAR BLDG.
FORT COLLINS, COLORADO 80523
USA
E-MAIL: mevin.hooten@colostate.edu

D. S. JOHNSON
J. M. LONDON
ALASKA FISHERIES SCIENCE CENTER
NATIONAL MARINE FISHERIES SERVICE
7600 SAND POINT WAY NE
SEATTLE, WASHINGTON 98115
USA

J. W. DURBAN
SOUTHWEST FISHERIES SCIENCE CENTER
NATIONAL MARINE FISHERIES SERVICE
NATIONAL OCEANIC
AND ATMOSPHERIC ADMINISTRATION
8901 LA JOLLA SHORES DRIVE
LA JOLLA, CALIFORNIA 92037
USA